Low-energy deposition of Co onto Co islands on Ag(100): Effect on submonolayer growth

J. Frantz, M. O. Jahma,* K. Nordlund, and I. T. Koponen

Accelerator Laboratory, P.O. Box 43, FIN-00014 University of Helsinki, Finland
(Received 8 March 2004; revised manuscript received 15 June 2004; published 18 February 2005)

Using classical molecular dynamics (MD) methods and rate equations, we have studied the effect of Co deposition onto a Co island at a Ag(100) surface. In the MD simulations, Co atoms were deposited on islands of sizes from 2×2 to 6×6 atoms with an energy of 25 eV at an incident angle of 20 degrees off normal. From the MD simulation results, we determined the functional form of the fragmentation kernel used in the rate equations as well as its parameters. The MD results also showed that irradiation-induced detachment from the island is common, while dissociation events of the island are very rare. Studying the growth process using rate equations, which included the restrictions deduced from the MD results, gave us island size distributions that agree with experimentally measured distributions. Thus, our results show that the submonolayer growth process can be explained solely by irradiation-induced detachment from the island.

I. INTRODUCTION

A large variety of techniques can be used to grow thin films. The techniques differ not only in their experimental setup but also in the quality of the resulting film. A promising but relatively little studied technique is deposition of hyperthermal adatoms and clusters on a surface. In this work, we will consider two hyperthermal methods; low-energy ion deposition (LEID) and ion-beam-assisted deposition (IBAD). In LEID, the surface is bombarded with ions with energies of 5–30 eV. The energy is high enough to induce the breaking up of islands and the creation of surface adatoms. These will contribute to an increase in nucleation centers for a new island, which will lead to a high surface island density. This high density is supposed to be the necessary condition for obtaining smooth layer-by-layer growth with LEID. IBAD techniques will give the same kind of layer-by-layer growth as LEID. However, with IBAD, the high island density is achieved by depositing the growing material thermally while at the same time bombarding the surface with high-energy immiscible ions that supposedly either break up the growing islands, or enhance detachment of adatoms on island edges and create new nucleation centers. Experiments with pulsed IBAD for Ag on Ag(111) and Cu on Cu(111) show that when a pulse of energetic particles is applied at the beginning of the growth of every new monolayer (ML), layer-by-layer growth is possible up to 7 ML.[1] The microscopic process of most importance behind all these methods seems to be enhanced detachment from island edges, as will be argued for in the present paper.

The growth of Co on Ag(001) films using LEID has been studied in recent experiments.[2] In these experiments, the morphology of the Co islands is found to be controlled by three different mechanisms: ion-impact-induced island fragmentation, pinning at surface-confined clusters, and ion-impact-induced island dissociation. It is concluded that the first two mechanisms contribute to an increased density of Co islands, while the third one decreases the island density.[2] It is, however, not clear how such massive mass redistribution as complete island dissociation could be induced by a single low-energy ion. In order to clarify these issues and settle the relative importance of the different processes suggested, we have studied these processes using computer simulations and present a model for the precursor of layer-by-layer growth in the submonolayer region. The case studied corresponds to conditions encountered in LEID.

The resulting high small-island density might be explained, apart from complete island dissociation, by detachment of adatoms from the edge of the islands caused by the energy transfer from the ion impacts, as we have suggested recently.[3] This would create an additional monomer flux onto the surface, and the necessary condition for that is that the flux should be proportional to some power of the length of the island perimeter and the density of islands of that size. In contrast to this, with fragmenting islands the small island density would not increase as much, because the parts of the fragmented islands tend to be of the same order in size on average, and the bigger the islands are, the rarer are the fragmentations of those islands. Thus, the resulting island size distribution would be very sharply peaked at the average island size. We have previously shown that the characteristic features of growth and in particular the form of island size distribution are uniquely characterized by these microscopic processes.[3,4] However, we have lacked the detailed justification for the basic assumptions of the model. In the present study, we provide the necessary microscopic details to justify the crucial hypothesis put forward in our previous work.

To get a complete picture of the processes governing growth using LEID, we need to identify the microscopic processes on the atomistic scale. To identify these processes, we need to utilize a tool which is capable of effectively and accurately measuring the positions of atoms during irradiation. The best candidate for this job is molecular dynamics (MD) simulations. Using MD simulations, we can follow the movement of single atoms as well as mimic the experimental conditions. Identifying the microscopic processes and their probabilities is, however, not enough; we also need to know how these processes will affect the growth in general and how they are reflected on the generic properties of growth. In order to study the growth process and draw inferences that are experimentally accessible, we utilize a rate equation model, which is a simplified and idealized description of the

growth process, yet fully justified in the present case of strongly reversible growth, where all spatial correlations are eliminated.[3,4] In the rate equation case, we insert the parameters deduced from the MD simulations, thus making them a semi-realistic description of growth under conditions encountered in LEID. The advantage of rate equations is that they make it possible to turn off certain microscopic processes, which makes it easy to deduce which parameters are important for the growth process.

This paper is arranged as follows. In Sec. II A we describe the method used in the MD simulations, the results of these simulations are presented in Sec. II B. We consider the rate equation simulation model in Sec. III A, the scaling of the distributions in Sec. III B, and the results of the rate equation simulations in Sec. III C. The obtained results are discussed in Sec. IV. We conclude the paper in Sec. V.

II. MICROSCOPIC SURFACE PROCESSES IN LEID

A. Molecular dynamics methods

Classical MD were used to study the atomistic processes during deposition. The simulation program uses the Gear V algorithm[5] to calculate atom trajectories and the Berendsen method[6] for temperature scaling.

In our model we consider a system consisting of a Ag substrate with a flat surface which has a square island of Co atoms consisting of one monolayer. The size of this island ranges from 2×2 atoms to 6×6 atoms. For islands smaller or equal to 25 atoms the used substrate has a total surface area 1069 Å^2, while for larger islands the size is 2033 Å^2. The square island has edges in the $\langle 110 \rangle$ directions, which is the energy minimum configuration for this type of islands. The dimensions of the smaller substrate is $8 \times 8 \times 4.5$ unit cells which corresponds to 1152 atoms and the size of the larger substrate is $11 \times 11 \times 4.5$ unit cells which corresponds to 2178 atoms. To create a system with one free surface, periodic boundaries were applied in the directions of the surface plane and nonperiodic boundaries were applied to the direction perpendicular to the surface plane. The three lowest monolayers of the substrate were fixed and a soft temperature scaling was applied on the following three monolayers.

To avoid thermal diffusion of the Co atoms, the system was simulated at an initial temperature of 77 K. To maintain this temperature, the atom velocities were scaled at the edges where periodic boundary conditions were applied. The incoming Co atom has a kinetic energy of 25 eV and hits the surface with an incident angle of 20 degrees off normal to mimic the experimental setup. All simulations were started from a thermalized substrate. The ϕ angle of the incoming atom was randomly chosen. The total length of one simulation was 5 ps.

The interaction between atoms in the system was described with the embedded-atom model (EAM) potential, the functional dependencies proposed by Johnson[7] were used. Model parameters for Ag can be found in Ref. 8 and the parameters for Co was obtained from the authors of a previous study of the same system.[9] Table I shows the values of the used potential parameters. The mixed Co-Ag interaction was obtained with the model proposed by Johnson,[7] this in-

TABLE I. The parameters for the interaction model used in the MD simulations.

Material	f_e	ϕ_e	α	β	γ
Ag	0.0118	0.4498	5.92	5.96	8.26
Co	0.0309	0.7232	5.25	6.96	9.28

teraction approximation has been validated by Hou *et al.* for both static and dynamic properties.[10]

Three different types of simulations were conducted. In the first type, the whole surface area was evenly bombarded. The results of this type are not relevant to the study; they were only used as a reference for the other results, and thus, they will not be presented explicitly in this paper. In the second type, the area of irradiation was set to five times the area of the island. The bombardment area is centered on the island, which gives us a relative bombardment area of 20% of the surface. The third type was used to gain more accuracy in the result statistics for the island detachment and fragmentation. This was done by limiting the area of irradiation to the island, which gives us a relative bombardment area of 100%; i.e., all of the bombarded atoms will hit the island. For all types of simulations, the point of impact was chosen randomly on the surface, taking the surface limiting conditions into account. Both the 20% and 100% limiting conditions gave similar results.

Five hundred events were simulated for all configurations. The third type was also simulated for 5000 cases to obtain maximum accuracy for the detachment results. The analysis of the simulation results was done at the end of each simulation with an analysis program specifically written for these simulations. In this analysis, a cluster of atoms or vacancies is defined as an entity in which all its parts are located within the distance $2 \times d_{nn}$ of each other, where d_{nn} is the nearest-neighbor distance for a relaxed lattice.

B. Molecular dynamics results

The analysis of the final configuration for the deposited atom was divided into nine different configurations in which the atom can be found after impact. The incoming atom can have landed on the surface, staying as a free atom on the surface. We label this configuration "On surface." If the atom has migrated to the edge of the island, we label the configuration "At island edge." If the incoming atom has switched places with a Co atom in the island, the configuration is labeled "In island," and if the switch has occurred with an Ag atom in substrate it is labeled "Ag exchange." If the incoming atom has undergone a "Ag exchange" within the island resulting in substrate Ag atoms in the island, the case is labeled "Ag exchange in island." Correspondingly, if the exchange is at the edge of the island, the case is labeled "Ag exchange at island edge." If the incoming atom just has been reflected off the surface, we label the case "Resputtered." If the incoming atom is a part of a fragmented cluster of the island at the surface, we label the case "In fragmented cluster." Tables II and III show the results for the different ex-

TABLE II. Results for the incoming atom. Cases A^*–H^* have the same parameters as given in Table IV. The number of different configurations are given in percent of the total number of events. The total number of events was 500. The parameters for the different cases are the same as in Table IV except for the relative bombardment area, which is 20% for these cases.

Configuration	A^*	B^*	C^*	D^*	E^*	F^*	G^*	H^*
On surface	29.9±3.2	28.2±1.0	27.6±1.7	23.8±2.9	21.8±2.9	19.0±1.3	16.2±1.5	28.7±3.0
Ag exchange	1.4±0.4	4.0±0.6	5.8±0.8	9.2±1.9	6.8±0.8	11.6±1.2	10.6±0.9	12.7±1.7
Ag exchange in island	7.6±0.7	6.0±1.3	4.8±0.9	4.8±0.8	4.2±1.1	5.0±0.8	6.2±1.0	3.8±0.8
Ag exch. at island edge	5.8±0.9	4.8±0.7	4.4±1.1	2.8±0.4	3.8±0.6	0.2±0.2	3.6±1.4	0.6±0.2
In island	22.6±2.2	26.4±1.4	30.0±1.9	26.8±2.3	34.6±1.6	37.4±1.5	38.0±1.0	30.8±2.8
At island edge	5.0±0.5	4.4±1.2	4.6±0.7	5.4±0.9	6.2±1.3	4.8±0.8	4.8±0.6	3.4±0.2
Resputtered	27.8±1.5	26.0±1.8	22.5±1.7	27.2±3.6	22.6±1.6	22.0±1.9	20.6±1.3	20.0±1.2
In fragmented cluster	0.0	0.2±0.2	0.2±0.2	0.0	0.0	0.0	0.0	0.0

amined cases, and Table IV describes the details of the different configurations.

In the analysis of the final configuration for the substrate, several different points of interest were identified, these are listed in Tables V and VI.

The "Ag adatom on surface" label indicates the occurrence of Ag adatoms on the surface not within two times the nearest-neighbor distance of the Co atom island. Note that multiple instances of this case does not necessarily mean that the adatoms form a cluster on the surface, although that is usually the case. If a Ag adatom is positioned next to the Co atom island, the configuration is labeled "Ag adatom at island edge" and if it is positioned in the island that is in the same layer as the Co atoms, the configuration is labeled "Ag adatom in island." If the adatom is located on top of the island it is labeled "Ag adatom on island." Sputtering of substrate atoms were also observed; the case of one sputtered Ag atom was labeled "Ag atom sputtered."

Two different final configurations for the Co atoms in the island were observed. The Co atoms can either be sputtered or fragmented from the island. The fragmentation of Co atoms from the island was observed as single atoms and as whole clusters of atoms. Single fragmented atoms are labeled "Co detached." Fragmented clusters of Co atoms are labeled as "cluster of X Co fragmented," where X indicates the number of Co atoms in the fragmented cluster.

To analyze the possible dissociation of the Co island, we also analyze the movement of atoms within the island itself.

The case labeled "Minor island disconfiguration" represents the case in which more than one atom but less than 20% of the total amount of island atoms have moved at least one nearest-neighbor distance. "Island disconfiguration" labels the case in which between 20% and 40% of the island atoms have moved at least one nearest-neighbor distance. If more than 40% of the island atoms have moved, we label the case "Major island disconfiguration." The criteria for island dissociation was that none of the resulting islands could be larger than 25% of the original island. In the simulations we ran, not one dissociation event was observed, and dissociation events are therefore not listed in the tables.

All errors for the data were calculated using the jackknife method.[11]

Figure 1 shows the total detachment probabilities for different island sizes. A curve of the form s^α has been fitted to the data, where the parameter α has a value of 0.38 ± 0.16 for the 20% relative bombardment area simulations and 0.52 ± 0.03 for the 100% relative bombardment area simulations.

It is interesting to note that a single impact moves the whole island ("island disconfiguration" events mentioned above), and that this occurs in more than 50% of the cases even for the largest island (see Tables V and VI). Several previous studies have examined adatom island movement by the diffusive motion of atoms along the edges.[12–15] The present results show that during IBAD or LEID conditions,

TABLE III. Results for the incoming atom. Cases A^{**}–H^{**} have the same parameters as given in Table IV. The number of different configurations are given in percent of the total number of events. The total number of events was 500. The parameters for the different cases are the same as in Table IV except for the relative bombardment area, which is 100% for these cases.

Configuration	A^{**}	B^{**}	C^{**}	D^{**}	E^{**}	F^{**}	G^{**}	H^{**}
On surface	31.2±0.6	22.3±0.7	20.0±0.5	14.6±0.5	14.5±0.6	9.1±0.4	8.9±0.4	12.1±0.4
Ag exchange	0.6±0.1	0.4±0.1	0.5±0.1	0.4±0.1	0.2±0.1	0.2±0.1	0.2±0.1	0.4±0.1
Ag exchange in island	8.9±0.4	10.2±0.5	5.0±0.3	7.5±0.4	6.0±0.3	6.3±0.4	5.7±0.3	4.8±0.3
Ag exchange at island edge	1.3±0.2	1.2±0.2	0.7±0.1	0.8±0.1	0.5±0.1	0.6±0.1	0.5±0.1	0.4±0.1
In island	35.0±0.7	48.3±0.8	57.1±0.7	61.5±0.6	68.5±0.8	69.0±0.7	75.2±0.6	74.0±0.6
At island edge	7.4±0.4	4.8±0.3	4.5±0.3	0.8±0.1	0.5±0.1	2.1±0.2	0.5±0.1	2.2±0.2
Resputtered	15.1±0.4	11.9±0.4	11.7±0.5	12.3±0.5	6.7±0.3	12.7±0.5	6.4±0.4	5.9±0.3
In fragmented cluster	0.5±0.1	0.8±0.1	0.5±0.1	0.1±0.1	0.1±0.1	0.0	0.1±0.1	0.2±0.1

TABLE IV. Substrate configurations used in the MD simulations.

Configuration	A	B	C	D	E	F	G	H
Island size (atoms)	2×2	2×3	3×3	3×4	4×4	4×5	5×5	6×6
Substrate size (Å²)	1069	1069	1069	1069	1069	1069	1069	2033
Island coverage (%)	3.13	4.69	7.04	9.39	12.51	15.62	19.65	14.81

not only the thermally activated motion but also the athermal impact-induced one needs to be considered.

Our results also show that there is an appreciable possibility of the incoming Co ion causing Ag entering the island. The results in Tables II and III (Ag exchange in island and at island edge) show that this probability is largest for the smallest (less than ten adatoms) islands, then remains about constant within the uncertainty at around 6% for the larger ones. Because of the atom size and chemical differences, an Ag atom in a Co island is likely to affect the island properties strongly. Similar to the ion-induced island motion effect, this mixing might also have to be accounted for in studies of adatom island mobility. It does seem to have a clearly smaller probability, though.

The fact that no island dissociation was observed is not a quite obvious result. Atom migration barriers on metal surfaces are typically of the order of 0.5 eV or less,[16] so that in principle it is energetically possible that a 25 eV ion could displace all atoms in the current small adatom islands leading to dissociation. This would, however, require a very even distribution of kinetic energy and momentum from the projectile to the adatoms, as well as requiring most of the momenta pointing outwards. That this is very improbable is confirmed by our results.

III. MODELING GROWTH

A. Rate equation model

The island growth with breakup of islands is a reversible process, and the systems of interest are affected by substan-

tial island mobilities.[3,4,17,18] This kind of growth can be described neglecting the spatial correlations between growing islands,[4,17–22] and thus can be modeled by using rate equations as a reversible aggregation-breakup process $A_i + A_j \rightleftarrows A_{i+j}$ of clusters of size i and j with the rates of aggregation and breakup specified by reaction rates $K(i,j)$ and $F(i,j)$, respectively.[18–22] The rate equations for the areal density n_s of islands of size $s \geq 1$ are now given by[4,23]

$$\frac{dn_s}{dt} = \frac{1}{2} \sum_{i+j=s} \left[K(i,j)n_i n_j - F(i,j)n_s \right]$$
$$- \sum_{j=1}^{\infty} \left[K(s,j)n_s n_j - F(s,j)n_{s+j} \right] + \Phi \delta_{1,s}, \quad (1)$$

where the source Φ is the deposition flux of adatoms in units of monolayers per second (ML/s).

The aggregation kernel for islands with diffusivity D_i is given by the Smoluchowski formula $K(i,j) = K_0(D_i + D_j)$, where we omit the logarithmic dependence on the island size.[19] This is consistent with the point island model used. In cases of interest to us, metallic clusters on a metal surface, the diffusion coefficients of the islands follow an inverse power law $D_i \propto i^{-\mu}$ with μ in the range $1 \leq \mu \leq 2$.[24] We restrict ourselves to models in which $\mu = 1$ or 2.

For fragmentation (or breakup) of an island of size $s = i + j$, the fragmentation rate is taken to depend on the island size $F(i,j) = F_0(i+j)^{\alpha-1}$, and only binary breakup is allowed. When only adatom detachment is allowed, the breakup rate

TABLE V. Results for the substrate. Cases A^*–H^* have the same parameters as given in Table IV. The number of different configurations are given in percent of the total number of events. The total number of events was 500. The parameters for the different cases are the same as in Table IV except for the relative bombardment area, which is 20% for these cases.

Configuration	A^*	B^*	C^*	D^*	E^*	F^*	G^*	H^*
Ag exchange	32.2±3.7	24.0±1.6	10.8±1.2	12.6±2.2	16.4±2.0	11.4±0.9	11.0±1.9	13.2±1.3
Single Ag adatom on surface	11.8±1.5	18.4±2.5	28.6±2.0	22.4±1.9	19.4±1.1	19.0±1.6	19.2±1.7	24.6±1.6
Two Ag adatoms on surface	0.6±0.4	0.8±0.2	0.0	1.2±0.4	0.4±0.2	1.0±0.3	0.8±0.5	2.6±1.6
Ag adatom at island edge	7.2±0.8	5.4±0.8	6.6±0.6	6.4±0.6	4.4±1.1	6.4±1.1	8.4±1.1	4.6±0.8
Ag adatom in island	53.5±4.4	46.4±3.7	34.6±1.4	35.8±2.1	40.2±1.3	33.8±1.8	38.2±1.6	33.8±1.2
Single Ag atom sputtered	3.8±1.3	5.2±0.7	3.6±0.5	3.2±0.9	3.8±0.7	4.8±0.6	3.8±0.9	5.0±0.8
Co detached	0.8±0.5	2.0±0.7	0.8±0.4	2.4±0.4	1.6±0.7	1.8±0.7	2.4±0.5	1.8±0.2
One cluster of two Co fragments	0.0	0.2±0.2	0.4±0.2	0.8±0.4	0.0	0.0	0.0	0.0
Minor island disconfiguration	35.6±2.1	41.4±2.4	57.8±2.1	54.8±1.4	54.4±2.6	58.2±1.1	64.1±2.2	63.0±2.2
Island disconfiguration	6.4±0.5	7.6±1.6	4.8±0.4	8.0±1.6	2.8±0.9	4.2±0.2	3.0±0.7	2.0±0.5
Major island disconfiguration	17.4±1.9	14.0±1.2	2.2±0.8	1.8±1.1	1.8±0.6	0.4±.2	0.4±0.2	0.0

TABLE VI. Results for the substrate. Cases $A^{**}-H^{**}$ have the same parameters as given in Table IV. The number of different configurations are given in percent of the total number of events. The total number of events was 500. The parameters for the different cases are the same as in Table IV, except for the relative bombardment area, which is 100% for these cases.

Configuration	A^{**}	B^{**}	C^{**}	D^{**}	E^{**}	F^{**}	G^{**}	H^{**}
Ag exchange	75.2 ± 1.3	71.6 ± 1.1	41.3 ± 1.1	44.4 ± 1.0	53.9 ± 1.2	49.6 ± 1.2	52.8 ± 1.1	49.0 ± 1.3
Single Ag adatom on surface	3.6 ± 0.3	4.1 ± 0.3	2.5 ± 0.2	3.3 ± 0.3	1.5 ± 0.2	2.3 ± 0.2	1.6 ± 0.2	1.2 ± 0.1
Two Ag adatoms on surface	0.0	0.1 ± 0.1	0.0	0.1 ± 0.1	0.0	0.0	0.0	0.0
Ag adatom at island edge	5.0 ± 0.3	4.6 ± 0.3	2.4 ± 0.2	2.0 ± 0.2	2.2 ± 0.2	1.9 ± 0.2	1.6 ± 0.2	1.6 ± 0.2
Ag adatom in island	86.1 ± 1.2	83.9 ± 1.2	52.5 ± 1.2	60.3 ± 1.2	64.2 ± 1.0	65.7 ± 1.3	66.6 ± 1.3	67.4 ± 1.3
Single Ag atom sputtered	0.4 ± 0.1	0.7 ± 0.1	0.1 ± 0.1	1.1 ± 0.2	0.1 ± 0.1	0.9 ± 0.1	0.1 ± 0.1	0.2 ± 0.1
One single Co sputtered	0.0	0.0	0.5 ± 0.1	0.0	0.0	0.2 ± 0.1	0.1 ± 0.1	0.1 ± 0.1
Co detached	5.0 ± 0.3	4.1 ± 0.3	3.0 ± 0.2	4.6 ± 0.3	8.0 ± 0.4	4.4 ± 0.3	7.5 ± 0.4	9.3 ± 0.3
One cluster of two Co fragments	0.6 ± 0.1	0.8 ± 0.1	0.7 ± 0.1	0.2 ± 0.1	0.3 ± 0.1	0.3 ± 0.1	0.2 ± 0.1	0.2 ± 0.1
Minor island disconfiguration	18.2 ± 0.6	25.8 ± 0.7	42.0 ± 0.8	47.2 ± 0.7	52.0 ± 0.7	61.6 ± 0.6	66.2 ± 2.3	74.1 ± 0.8
Island disconfiguration	11.8 ± 0.5	12.9 ± 0.4	17.1 ± 0.6	20.4 ± 0.6	18.2 ± 0.6	13.6 ± 0.5	12.8 ± 0.5	7.7 ± 0.4
Major island disconfiguration	38.2 ± 0.7	34.7 ± 0.6	8.2 ± 0.4	6.4 ± 0.3	6.1 ± 0.3	2.6 ± 0.2	1.6 ± 0.2	0.3 ± 0.1

of adatoms is given by $F(i,j)=F_0'(i+j)^{\alpha}(\delta_{i1}+\delta_{j1})$, where the δ_{ij} restricts breakup to adatoms only. In both cases, α is related to the geometry of the islands characterizing how impacts are assumed to affect the breakup.[25,26] The detachment constant on the lattice is defined as $F_0'=L^2 F_0$, where L^2 is the size of the system (in the simulations we used $L^2 =250\,000$ lattice sites) and F_0 is the detachment rate in number of detachments per second. The MD simulations performed here show definitely that fragmentation is not likely to occur, but enhanced detachment takes place. Moreover, the detachment depends on the size of the islands as expected, i.e., it is proportional to length of the island perimeter.

In order to study the dynamics of island growth described by Eq. (1) without any additional assumptions concerning scaling or stationarity, we have simulated island growth using the particle coalescence method (PCM).[4,21] In this simplified model reaction, kernels in the rate equations can be specified exactly since the geometric effects arising from the complicated morphology of real islands are not taken into account (see Ref. 4 and references therein).

B. Scaling of the distributions

In defining the appropriate scaling of the island size distributions, we use the probability density that an atom selected at random is contained in an island of size s, $p(s,\theta) =sn_s(\theta)/\Sigma_{s=1}^{\infty}sn_s(\theta)=sn_s(\theta)/\theta$, and define the average size of the island as the first moment of this distribution $\bar{s}(\theta) =\Sigma_s sp(s,\theta)$. Among different possibilities to define scaling functions, this choice is convenient to resolve the scaling properties of interest here.[3,4,27] After the initial transient stage the mean size of the island becomes the only important scale determining the behavior of the system. The island size distribution then scales as[27] $g(s/\bar{s})=\bar{s}p(s,\theta)$, which is now independent of the coverage θ and of the parameters $R =K_0/\Phi$ and $\kappa=F_0/K_0$.[27,28] The island size distribution is de-

termined completely by $g(x)$ provided the average size $\bar{s}$ is specified. In what follows, the size distribution is of most interest, because its generic form is characteristic to the nature of reversibility; either a fragmentation process or a detachment of adatoms occurs.[3,4]

C. Rate equation model results

The scaling functions $g(x)$ corresponding to the models of fragmentation and enhanced detachment were monitored in PCM simulations until parameter-independent limiting shapes were attained. For fragmentation with homogeneous breakup kernels, the scaling function $g(x)$ can be fitted with
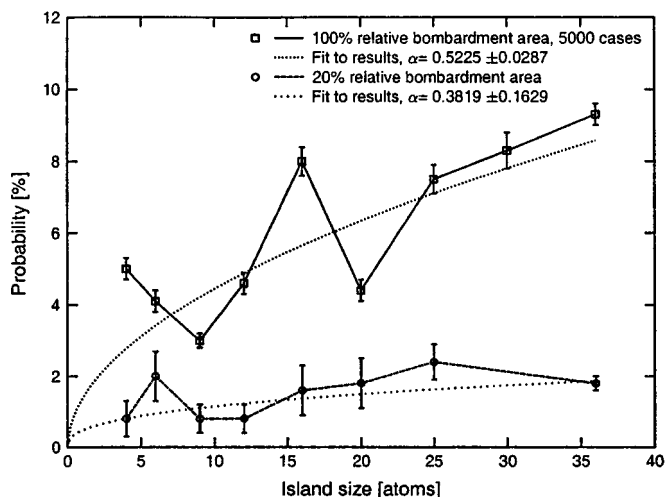

FIG. 1. The detached Co atoms for the configuration with 100% relative bombardment area. A curve with a function of $F=Cs^{\alpha}$ has been fitted to the data, where C is a scaling factor and s the size of the island. The 100% relative bombardment area curve shows data of 5000 events and can thus not be compared directly to the data in Table VI.
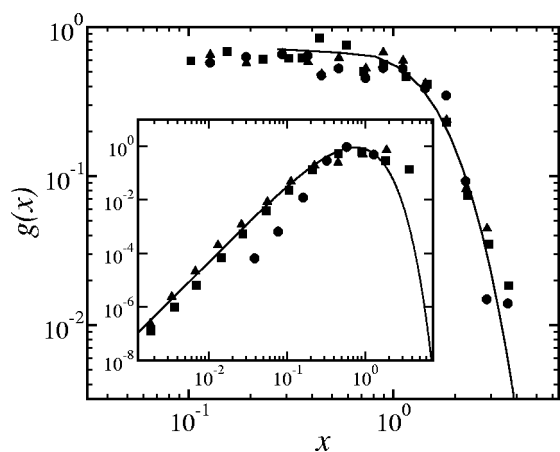
FIG. 2. Scaled distribution from our simulation results for aggregation with adatom detachment only compared with LEID experiments (Ref. 2) with deposition energies of 15 eV (circles), 25 eV (triangles), and 30 eV (squares). The solid line corresponds to the fit to the scaling function for the case $(\mu,\alpha)=(2,1/2)$ and $R=10^6$, $\kappa=4.0\times10^{-7}$. In the inset, the scaled distribution from our simulations for aggregation with fragmentation is compared with IBAD experiment (Ref. 29), with bombarding energies 400 eV (triangles), 4 keV (squares), and vapor deposition (circles). The solid line corresponds to the fit to the scaling function for the case (2,1).

the exponential-type function[23] $g_f(x)\propto x^{\delta_f}\exp(-cx)$, where values of δ_f are sensitive to both homogeneity exponents α and μ, and is given with good accuracy by relation $\delta_d=\alpha+\mu$, as we have previously shown for this class of models.[4]

For adatom detachment only, the properties of the growth differs from that with island fragmentation in a fundamental way. With increasing values of the parameter κ there is a transition to the region of regular growth with island size distributions of scaling form with an anomalously high density of small islands.[3] This observation holds for other models with $\mu=3/2$ and 1 and $\alpha=1/2$ or 1. For island-size-independent detachment with $\alpha=0$, there is no detectable transition in the parameter range accessible to PCM simulations.

For enhanced detachment, the scaling function $g(x)$ contains an exponential residue at the leading edge, which is due to singular island number density distribution of small islands behaving as $n(x)\propto1/x$ [from equations of the Sec. III B we see that $g(x)\propto xn(x)$]. The scaling function for enhanced detachment can be fitted with the modified exponential function, $g_d(x)=Ax^{\delta_d}\exp(-cx)+B\exp(-x/x_0)$, where exponential residue with $x_0\approx0.2$ represents the contribution from the small islands due to a random (Poissonian) aggregation of small islands. The values of the exponent δ_d for the studied models seem to correspond to the prediction $\delta=\alpha+\mu$ based on the aggregation/fragmentation model.[3]

In case of IBAD, the scaled island size distributions can be inferred from the results of Esch *et al.*[29] [IBAD of Pt on Pt(111)]. These are compared in Fig. 2 (inset) with the predictions of our model. It is evident that the IBAD experimental results are entirely different from the distributions obtained for adatom detachment only or with very small breakup, but they do compare favorably with the distribu-

tions corresponding to sufficiently large probabilities for the fragmentation of islands. However, in case of experimental results by Esch *et al.*, additional nucleation centers are created, which leads to behavior similar to fragmentation. Although for IBAD the shape of the scaling function $g(x)$ would not be a conclusive argument favoring fragmentation only, it can be used here to show that fragmentation nevertheless leads to a characteristic shape of the scaling function, entirely different from that observed in detachment only.

In the LEID experiments reported by Degroote *et al.*,[2] the island size distributions indicate an anomalously high density of small islands, in sharp contrast to those obtained in IBAD. Moreover, now the shape of distribution is such that neither fragmentation nor enhanced creation of nucleation centers can explain it. The island size distributions for enhanced adatom detachment obtained from PCM simulations are compared in Fig. 2 with the experimental data results by Degroote *et al.*,[2] where distribution from LEID have been reported. In the experiments conducted by Degroote, an anomalously high small-island density is observed, and it is attributed to island fragmentation, although other possibilities such as pinning at surface-confined clusters leading to an increased island density are also considered. Under the conditions studied by Degroote, complete island dissociation is ruled out, since it would lead to a decrease of island density. Of all known microscopic effects, only the enhanced detachment thus remains. The only remaining plausible explanation for the experimental results is thus the enhanced detachment of adatoms, the rate depending on the perimeter of the island size. This is concluded on the basis that MD simulations indicate a parameter $\alpha\approx0.5$ in the present case, and when used in the model of growth.

Under these conditions, the effect of detachment is to create an additional flux of adatoms originating from the large islands. As the mean island size grows, the flux of adatoms increases and thus promotes the growth of the small island part of the size distribution. This can be seen in the size distribution as an additional exponential tail if compared to the case of fragmenting islands, where the distribution does not have a similar high small-island density. Only with these assumptions PCM simulations yield distributions in good agreement with experimental results.

IV. DISCUSSION

Our simulations, which correspond closely to the energy region of LEID applied in experiments by Degroote *et al.*, are rather conclusive with respect to the microscopic process; we cannot, however, detect a single instance of island dissociation, and island fragmentation also seems to be a relatively rare event. Instead, the dominant mechanism is either the enhanced detachment of adatoms or several consecutive fragmentation/detachment events eventually leading to several detached adatoms. The total effect of these events is rather well described by a detachment kernel with $\alpha=1/2$. It is just this kind of kernel that uniquely leads to a stationary, scaling form of island size distribution typical to LEID characterized by a simple exponential leading part.

PCM simulations show that with values of α confined near 0.5, we will always have the exponential leading edge,

which is also the characteristic feature of the experimental results. With significantly higher values of α, the scaling of distributions in the submonolayer region is lost and the approach to scaling form is very slow. Moreover, there is a tendency to extremely slow growth in time, and a power-law-type leading edge of the scaling distribution when $\alpha = 1$ is approached. On the other hand, with adatom detachment only, values significantly smaller than 0.5 will lead to faster growth, and with decreasing α, scaling function $g(x)$ rapidly begins to resemble the case for fragmentation. We can thus conclude that the exponential leading edge really is a characteristic feature related to enhanced detachment depending on the perimeter of the island.

In our previous work, we studied in more detail the nature of the transition that leads to anomalously high island density.[3] With increasing detachment rate there is a relatively sharp transition to regular submonolayer growth[3] with an anomalously high density of small islands. What makes the present results particularly interesting is that the transition to the new regular growth mode sets in within a parameter range corresponding very closely to that found to be useful in hyperthermal deposition experiments. We expect that the predictions here could be easily checked with well-controlled experiments.

V. CONCLUSIONS

Our aim in this study was to understand the formation process of the island density and size distribution observed in experiments. To be able to answer this question, we used two different approaches. Molecular dynamics simulations were used to identify the atomistic processes that the substrate undergoes during irradiation and their probabilities of occurrence. Using the the probabilities of these processes, we were able to simulate the island densities and size distributions using PCM simulations.

Using the data deduced from the MD results, we were able to calculate the scaling parameter α, as well as to confirm $F_0 s^\alpha$ as the functional form of the fragmentation kernel. α was found to have values of 0.38 ± 0.16 and 0.52 ± 0.03 depending on the limiting conditions used. These values are consistent with the previously assumed value of 0.5 obtained from the simple geometrical argument that the detachment probability scales as the side length of the island.

The results of PCM simulations show that enhanced adatom detachment leads to regular growth with an anomalously high island density. In that regular growth mode the island size distributions are of scaling form and the average island size and mean island density follow a power law with well defined effective scaling exponents. At present, the nature and properties of this transition are not completely understood.

Comparison of PCM simulations with available experimental results for island size distributions obtained in hyperthermal deposition suggests that in high energy deposition methods such as ion-beam-assisted deposition fragmentation of islands may affect the growth, while in low-energy ion deposition the enhanced adatom detachment is operative. An anomalously high density of small islands and slow growth of the mean size of islands is found in models in which enhanced adatom detachment occurs with a ratio of bombardment to deposition around 0.01 to 0.1. These results and the parameter region, where growth with well defined scaling properties occurs, correspond closely to the values found useful in LEID experiments.

Taken together, the MD and PCM simulation results have shown that detachment from the islands is enough to explain the experimentally observed island density and size distribution. Previously, it was believed that dissociation of the islands is the main contributor to this; however, we did not observe a single dissociation event in the MD simulations. Hence, it was not taken into account in the PCM simulations. Since the results of the PCM simulations agree well with the experimental results, we can conclude that the dissociation of islands is not a significantly contributing process.

*Laboratory of Physics, P.O. Box 1100, University of Technology, FIN-02015 HUT, Espoo, Finland.

[1] G. Rosenfeld, N. N. Lipkin, W. Wulfhekel, J. Kliewer, K. Morgenstern, B. Poelsema, and G. Comsa, Appl. Phys. A: Mater. Sci. Process. **61**, 455 (1995).

[2] B. Degroote, A. Vantomme, H. Pattyn, and K. Vanormelingen, Phys. Rev. B **65**, 195401 (2002).

[3] I. T.Koponen, M. Jahma, M. Rusanen, and T. Ala-Nissila, Phys. Rev. Lett. **92**, 086103 (2004).

[4] M. Rusanen, I. T. Koponen, and J. Asikainen, Eur. Phys. J. B **36**, 567 (2004).

[5] C. W. Gear, *Numerical Initial Value Problems in Ordinary Differential Equations* (Prentice-Hall, Englewood Cliffs, NJ, 1971).

[6] H. J. C. Berendsen, J. P. M. Postma, W. F. van Gunsteren, A. DiNola, and J. R. Haak, J. Chem. Phys. **81**, 3684 (1984).

[7] R. A. Johnson, Phys. Rev. B **41**, 9717 (1990).

[8] R. A. Johnson, Phys. Rev. B **39**, 12 554 (1989).

[9] M. Hou (private communication).

[10] M. Hou, M. El Azzaoui, H. Pattyn, J. Verheyden, G. Koops, and G. Zhang, Phys. Rev. B **62**, 5117 (2000).

[11] R. G. Miller, Biometrika **61**, 1 (1974).

[12] J. Heinonen, I. Koponen, J. Merikoski, and T. Ala-Nissilä, Phys.

Rev. Lett. **82**, 2733 (1999).

[13] A. F. Voter, Phys. Rev. B **34**, 6819 (1986).

[14] W. W. Pai, A. K. Swan, Z. Zhang, and J. F. Wendelken, Phys. Rev. Lett. **79**, 3210 (1997).

[15] S. V. Khare, N. C. Bartelt, and T. L. Einstein, Phys. Rev. Lett. **75**, 2148 (1995).

[16] H. Brune, Surf. Sci. Rep. **31**, 121 (1998).

[17] J. Heinonen, I. Koponen, J. Merikoski, and T. Ala-Nissilä, Phys. Rev. Lett. **82**, 2733 (1999).

[18] P. A. Mulheran and D. A. Robbie, Phys. Rev. B **64**, 115402 (2001).

[19] P. L. Krapivsky, J. F. F. Mendes, and S. Redner, Eur. J. Biochem. **4**, 401 (1998).

[20] P. Meakin and M. H. Ernst, Phys. Rev. Lett. **60**, 2503 (1988).

[21] K. Kang and S. Redner, Phys. Rev. A **30**, 2833 (1984).

[22] H. Wright and D. Ramkrishna, Phys. Rev. E **47**, 3225 (1993).

[23] I. T. Koponen, M. Rusanen, and J. Heinonen, Phys. Rev. E **58**, 4037 (1998).

[24] A. F. Voter, Phys. Rev. B **34**, 6819 (1986).

[25] J. Jacobsen, B. H. Cooper, and J. P. Sethna, Phys. Rev. B **58**, 15 847 (1998).

[26] J. M. Pomeroy, J. Jacobsen, B. H. Cooper, and J. P. Sethna, Phys. Rev. B **66**, 235412 (2002).

[27] G. S. Bales and D. C. Chrzan, Phys. Rev. B **50**, 6057 (1994).

[28] C. M. Sorensen, H. X. Zhang, and T. W. Taylor, Phys. Rev. Lett. **59**, 363 (1987).

[29] S. Esch, M. Breeman, M. Morgenstern, T. Michely, and G. Comsa, Surf. Sci. **365**, 187 (1996).